J Mol Neurosci (2015) 57:97–105
DOI 10.1007/s12031-015-0582-x

Pulsed Radiofrequency Treatment Enhances Dorsal Root Ganglion Expression of Hyperpolarization-Activated Cyclic Nucleotide-Gated Channels in a Rat Model of Neuropathic Pain

Yiming Liu[1] · **Yi Feng**[1] · **Tingjie Zhang**[1]

Received: 29 September 2014 / Accepted: 18 May 2015 / Published online: 28 May 2015

Abstract Pulsed radiofrequency (PRF) treatment is a minimally invasive technique with multiple therapeutic applications. Hyperpolarization-activated cyclic nucleotide-gated (HCN) channel mediating Ih may regulate neuropathic pain signaling. This study aimed to determine whether PRF suppresses neuropathic pain by altering HCN channel expression in dorsal root ganglion (DRG) neurons. Male Sprague Dawley rats with sciatic nerve chronic constriction injury (CCI) were randomly assigned to PRF (n=60) and sham control (n=60) groups, respectively. On postoperative day 7 (D07), PRF or sham treatment was delivered to the proximal sciatic nerve for 8 min. Behavioral tests were performed before surgery (D0), on D07, and on D1, D7, and D14 after PRF or sham treatment. HCN1 and HCN2 expression levels in the DRG were examined by immunohistochemistry and Western blot. The results showed that thermal hyperalgesia, mechano-allodynia, and mechano-hyperalgesia were lower, and DRG expression levels of HCN1 and HCN2 higher, in the PRF group compared with sham control animals (all P<0.05 at D14). In conclusion, PRF can upregulate HCN channel expression in the DRG of rats with sciatic nerve CCI. How this regulation of Ih in nociceptive afferents contributes to the suppression of neuropathic pain by PRF remains to be determined.

Keywords Hyperpolarization-activated cyclic nucleotide-gated channel · Pulsed radiofrequency · Neuropathic pain · Chronic constriction injury · Neuromodulation

✉ Tingjie Zhang
zhangtjmedsci@163.com

[1] Pain medicine department, Peking University People's Hospital, No. 11, Xizhimen South Street, Xicheng District, Beijing 100044, China

Introduction

Peripheral or central nerve injury often leads to neuropathic pain characterized by thermal hyperalgesia, mechano-hyperalgesia, mechano-allodynia, and spontaneous pain (Vranken 2012). The pathogenesis of neuropathic pain involves multiple neuroplastic mechanisms, and this mechanistic complexity has hampered the development of broadly effective treatments. Peripheral and central sensitization of nociceptive pathways is critical to the development and maintenance of neuropathic pain (Vranken 2012; Kerstman et al. 2013). Spontaneous ectopic discharges from the site of injury and dorsal root ganglia (DRG) are a result of peripheral sensitization and may kindle the sensitization of spinal nociceptive pathways (Chung et al. 2002; Wan 2008).

Changes in the expression or kinetic properties of ion channels in nociceptive pathways, such as sodium, calcium, and transient receptor potential vanilloid 1 (TRPV1) channels, are closely associated with neuropathic pain (Hains et al. 2004; Li et al. 2004). Recently, a hyperpolarization-activated cyclic nucleotide-gated (HCN) channel that generates a hyperpolarization-activated current (Ih) in the sinoatrial node was shown to be widely expressed in both the central and peripheral nervous systems (CNS and PNS, respectively) (Xiao et al. 2004), and the various members of the HCN channel family are now thought to play physiologic roles in a variety of cellular processes (Biel et al. 2009; Postea et al. 2011; He et al. 2014). Preclinical studies in animals have demonstrated the involvement of HCN channels in neuropathic pain (Chaplan et al. 2003; Jiang et al. 2008; Wickenden et al. 2009; Mazo et al. 2013), raising the possibility that these channels could be potential targets for therapeutic intervention. For example, increased expression of HCN1 and HCN2 and a shift in the activation curve of Ih have been reported to occur in a rat model of neuropathic pain (Du

et al. 2013a, b), while HCN2 knockout mice have been found to show no neuropathic pain, in response to thermal or mechanical stimuli, after a nerve lesion (Emery et al. 2011). Furthermore, pharmacologic inhibition of Ih in peripheral nociceptive neurons has been observed to reduce mechanical allodynia and thermal hyperalgesia in animal models of neuropathic pain (Du et al. 2013a; Tibbs et al. 2013; Young et al. 2014), alleviate inflammation-induced hypersensitivity of the rat temporomandibular joint (Hatch et al. 2013), and augment activity-dependent conduction velocity slowing in axotomized C-fibers (Mazo et al. 2013). Thus, there is substantial evidence that enhanced HCN channel function may contribute to neuropathic pain.

Pulsed radiofrequency (PRF) is a novel therapeutic modality for pain management. Electromagnetic waves (20 ms, 500 kHz) are applied close to the DRG or dysfunctional peripheral nerve to increase the mean local temperature to a maximum of 42 °C. In 1996, Sluijter introduced PRF into clinical practice and first reported the effects of PRF on DRG excitability and nociceptive transmission (Sluijter 2005). Subsequent clinical studies demonstrated therapeutic efficacy against neuropathic pain. For example, Zundert et al. reported significant pain reduction in all study patients with idiopathic trigeminal neuralgia (Van Zundert et al. 2003), Cohen et al. found PRF to the DRG superior to pharmacologic management for the treatment of chronic postsurgical chest pain (Cohen et al. 2006), and Ke et al. reported encouraging results in patients with thoracic postherpetic neuralgia (Ke et al. 2013). Moreover, PRF also reduces nociceptive responses in animal models. Tanaka et al. demonstrated that PRF of the rat sciatic nerve significantly reduces mechano-allodynia induced by resiniferatoxin (Tanaka et al. 2010), Aksu et al. found that PRF significantly decreases mechano-hyperalgesia in rabbits after tight ligation of the sciatic nerve (Aksu et al. 2010), and Perret et al. reported that PRF to the DRG decreases allodynia in rats with chronic constriction injury (CCI) to the L5 spinal nerve (Perret et al. 2011). In rats with L5 spinal nerve ligation (SNL), Park et al. found that PRF decreases mechano-hypersensitivity (Park et al. 2012). Despite confirmed efficacy in multiple neuropathic pain models and clinical studies, the anti-nociceptive mechanisms of PRF remain unclear.

Based on the relationship between HCN channel activity and neuropathic pain reported previously and the known efficacy of PRF against neuropathic pain, we hypothesized that decreases in HCN channel expression may underlie (at least in part) the anti-nociceptive effect of PRF. In the present study, we explored this possibility by applying PRF to rats with sciatic nerve CCI and measuring the changes in HCN1 and HCN2 expression in the DRG.

Materials and Methods

All surgical and experimental procedures were performed in accordance with the International Association for the Study of Pain (IASP) ethical guidelines for the investigation of experimental pain in conscious animals, and approved by the Medical Ethics Committee of Peking University People's Hospital, China.

Animals

A total of 120 male Sprague Dawley rats weighing 200–220 g were used (Vital River Laboratories, Beijing, China). The rats were housed in cages with corncob bedding under a reverse 12 h light–dark cycle and provided ad libitum access to food and water.

Sciatic Nerve CCI model

Rats were anesthetized by intraperitoneal injection of 40 mg/kg sodium pentobarbital. The skin of the right thigh was shaved and sterilized with 0.2 % Anerdian. The right common sciatic nerve was exposed at the mid-thigh level, and four loosely constrictive ligatures of 4-0 chromic gut were tied around the nerve with about 1 mm spacing between knots. The knots were tightened slowly until a brief twitch in the hindlimb was observed. After washing, the incision was sutured layer-by-layer with 4-0 silk thread and the animal allowed to recover from anesthesia (Bennett et al. 1988).

Pulsed Radiofrequency Application

The rats used for the CCI model were assigned to either a PRF group (n=60) or a Sham control group (n=60) using a random number table, to be subjected to PRF or sham control treatment, respectively. On the seventh postoperative day (D07), a radiofrequency electrode (MG-230, Baylis, Canada) was placed on the skin adjacent to the proximal sciatic nerve (Fig 1). In the PRF group, PRF was delivered for 8 min using a pulse duration of 20 ms (500 kHz) and a pulse rate of 2 Hz, so as to achieve a local tissue temperature of 42 °C. In the Sham group, the RF electrode was placed at the same position for 8 min, but no radiofrequency current was administered (Fig. 1).

Behavioral Tests

Behavioral tests were performed before surgery (D0), 7 days after surgery (D07), and 1, 7, and 14 days after PRF/sham treatment (D1, D7, and D14). All testing was performed at the same time of the day (8:00–12:00 a.m.) in a quiet environment and was conducted by an investigator blinded as to whether the animal was in the PRF or Sham group.

Fig. 1 Pulsed radiofrequency delivered to the proximal sciatic nerve in a rat with sciatic nerve CCI. The electrode was placed adjacent to the proximal sciatic nerve. Current was delivered through the electrode (pulse duration, 20 ms; pulse rate, 2 Hz; local tissue temperature, 42 °C; duration, 8 min) to rats in the PRF group, but not to those in the Sham group

Paw Withdrawal Latency

Paw withdrawal latency (PWL) was induced and latency measured using a thermal stimulus apparatus (BME410, Chinese Academy of Medical Sciences Institute of Biomedical Engineering, Beijing, China), as described by Hargreaves (Hargreaves et al. 1988). Rats were placed in individual clear plastic cages and allowed to acclimate for 30 min. The heat stimulus was focused on the plantar surface of the right hindpaw. The intensity of the heat stimulus was adjusted to evoke a baseline PWL of 8 s in naïve animals. A 30 s cut-off was used to prevent tissue damage. Three PWL measurements were acquired at 5 min intervals and averaged to yield the reported values.

Paw Withdrawal Threshold (PWT)

Rats were placed individually in clear plastic cages on an elevated wire mesh table and allowed to acclimate for 30 min. Mechano-allodynia and mechano-hyperalgesia were assessed using two von Frey filaments (4 and 15 g), as described previously (Flatters et al. 2004). Each filament was applied five times to the mid-plantar area of the right hindpaw at 5 s intervals, and the mean frequency of withdrawal was recorded. Naïve rats almost never withdrew from 4 g stimulation, so a withdrawal frequency significantly >0 % at 4 g indicated mechano-allodynia. Naïve rats exhibited a withdrawal frequency of ~20 % in response to 15 g, so a higher mean withdrawal frequency was defined as mechano-hyperalgesia.

Western Blot Analysis

Six rats from each group were sacrificed after behavioral testing on D0, D07, D1, D7, and D14. The right L4–6 dorsal root ganglia were quickly removed and immersed in liquid nitrogen. After protein extraction, the bicinchoninic acid (BCA) assay was used to determine lysate protein concentrations. Proteins were separated on sodium dodecyl sulfate polyacrylamide gel electrophoresis (SDS-PAGE) gels and transferred to polyvinylidene difluoride (PVDF) membranes. After blocking with 5 % non-fat dried milk, membranes were incubated overnight at 4 °C with mouse monoclonal anti-HCN1 (5 μg/mL) or anti-HCN2 (5 μg/mL) antibodies (Abcam, Cambridge, UK) in Tris-buffered saline with Tween-20 (TBST) plus 5 % non-fat dried milk. After washing with TBST, the membranes were incubated with a horseradish peroxidase (HRP)-conjugated goat anti-mouse secondary antibody (Jackson Immune, West Grove, PA, USA) diluted in TBST plus 5 % non-fat dried milk. The immunolabeled protein bands were visualized using a chemiluminescence kit (ECL Western blot detection agents; Amersham Biosciences, UK). Blots were scanned with ImageQuant Las 4000 (GE Healthcare, Tokyo, Japan), and band densities quantified and compared using the Multi Gauge V3.2 software. Target protein band density was normalized to that of β-actin.

Immunohistochemistry

At each time point (D0, D07, D1, D7, and D14), six rats from each group were sacrificed after behavioral testing had been carried out. After opening the chest, 200 mL of normal saline were perfused through the aorta, followed by 200 mL of 4 % paraformaldehyde (PFA) in 0.1 mol/L phosphate-buffered saline (PBS, pH 7.4). The right L4–6 DRG were removed, post-fixed in PFA, and cryo-protected overnight in 10 mmol/L PBS plus 30 % sucrose. The ganglia were then cut into 2-μm thick serial sections on a cryostat (Leica, Wetzlar, Germany). After antigen repair with EDTA (pH 8.0) for 20 min, the sections were incubated overnight, in a humid chamber at 4 °C, with mouse monoclonal anti-HCN1 (2 μg/mL, Abcam, UK) or anti-HCN2 (10 μg/mL, Abcam, UK) antibody in TBST. Immunolabeled sections were then incubated with HRP-conjugated goat anti-mouse IgG (Zhongshan Golden Bridge Biotechnology Co., Ltd, Beijing, China) for 20 min, visualized with diaminobenzidine (DAB), and photographed under a light microscope (Olympus, Tokyo, Japan). For quantitation, cells with brown dots in the plasma membrane or cytosol were considered HCN positive; for each slide, three fields were randomly selected to determine the average optical density, which represents the expression intensity of HCN channel, using the Leica imaging software (Imaging Analysis Center for Peking University Health Science Center).

Data Analysis

Statistical tests were performed using the STATA 13.0MP software (StataCorp LP, College Station, TX, USA). Data from each group are mean±standard error of the mean

(SEM). Data were analyzed by mixed-effects restricted maximum likelihood (REML) regression. For intra-group comparison of time effect, Bonferroni multiple comparison correction was used to correct the P value threshold for multiple comparisons. After correction, the significance level was set as $P=0.005$ (0.05/10). Otherwise, $P<0.05$ was considered statistically significant.

Results

Effects of PRF Treatment on Behavioral Pain responses

Thermo-hyperalgesia

The PWL, in response to noxious heat, measured prior to surgery (D0, baseline) did not differ between rats assigned to receive CCI followed by PRF (PRF group) and those assigned to receive CCI followed by sham treatment (Sham group). The PWL measured on the 7th day following sciatic nerve CCI (D07) was significantly shorter in both groups relative to baseline (D0) ($P<0.005$), indicating thermo-hyperalgesia, but PWL did not differ significantly between groups (Fig. 2). However, in the days following PRF, PWL rose steadily, indicating reversal of CCI-induced hyperalgesia; in contrast, PWL remained lower than that of the baseline in the Sham group (sham PRF). The PWL of the PRF group was significantly higher than that of the Sham group over the post-PRF period (D1–D14; $P<0.05$) and at each post-PRF time point ($P<0.05$).

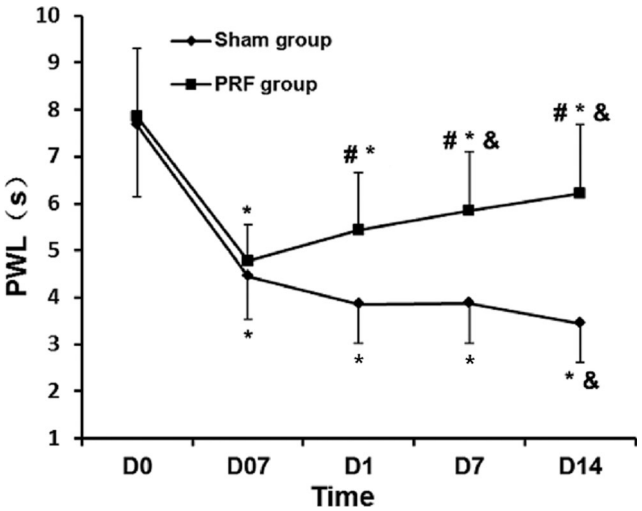

Fig. 2 Changes in paw withdrawal latency (PWL) in the Sham and PRF groups ($n=12$ rats per group). After CCI (D07), the PWL decreased in both groups, indicating thermo-hyperalgesia. After PRF (from D1 to D14), the PWL of the PRF group began to increase, consistent with reversal of CCI-induced hyperalgesia. In contrast, PWL continued to decrease in the Sham group, indicating progressively worsening hyperalgesia. Data are presented as the mean±SEM. $^{\#}P<0.05$, PRF group vs. the sham group at each time point using mixed-effects REML regression; $^{*}P<0.005$ within groups compared to D0 using mixed-effects REML regression, adjusted using Bonferroni multiple comparison correction; $\&P<0.05$ within groups compared with D07 using mixed-effects REML regression, adjusted using Bonferroni multiple comparison correction

Mechano-allodynia and Mechano-hyperalgesia

To measure possible changes in mechano-allodynia, we used 4 g von Frey filaments, which induce only non-painful mechano-stimulation in naïve rats (Fig. 3a). At baseline (D0), there was no significant difference in response rates between rats assigned to the PRF and Sham groups. The mean response rate increased significantly in both groups at D07 compared to baseline ($P<0.005$), indicating CCI-induced mechano-allodynia (with no difference between the two groups). After PRF (D1-D14), the mean response rate decreased progressively and was not significantly different from the baseline value at D14. In the Sham group, however, the mean response rate remained elevated and did not differ significantly from that of D07 at any time point. The mean response rate of the PRF group was significantly lower than that of the Sham group at D7 and D14 ($P<0.05$). Thus, PRF reversed CCI-induced mechano-allodynia.

Mechano-hyperalgesia was measured by paw withdrawal frequency in response to a 15 g von Frey filament. The mean paw withdrawal frequency did not differ between the two groups at baseline (D0). Withdrawal frequency increased significantly in both the PRF and Sham groups at D07 after CCI ($P<0.005$), indicating marked CCI-induced mechano-hyperalgesia (Fig. 3b), with a slightly higher mean response rate observed in the PRF group. After PRF (D1–D14), the mean response rate in the PRF group decreased significantly compared to D7, although it remained higher than baseline at D14. Thus, PRF partially reversed CCI-induced mechano-hyperalgesia. In contrast, the mean response rate in the Sham group continued to rise modestly over the D1–D14 period, indicating no change or even slightly higher mechano-hyperalgesia. The overall response rate was significantly lower in the PRF group than in Sham animals over the entire posttreatment period ($P<0.05$) and at each time point ($P<0.05$).

Distribution of HCN1 and HCN2 Expression in Dorsal Root Ganglia

HCN1 was detected on the plasma membrane in all large- and medium-sized DRG neurons (Fig. 4). HCN2 was also detected in all DRG neurons, but mainly in the cytoplasm of medium- and small-sized DRG neurons (Fig. 5). Seven days after neuropathic pain induction (D07), HCN1 and HCN2 expression levels were significantly decreased in both sham and PRF groups (all $P<0.005$) without significant inter-group differences ($P>0.05$). In the sham group, HCN1 and HCN2 expression levels did not significantly change at later time

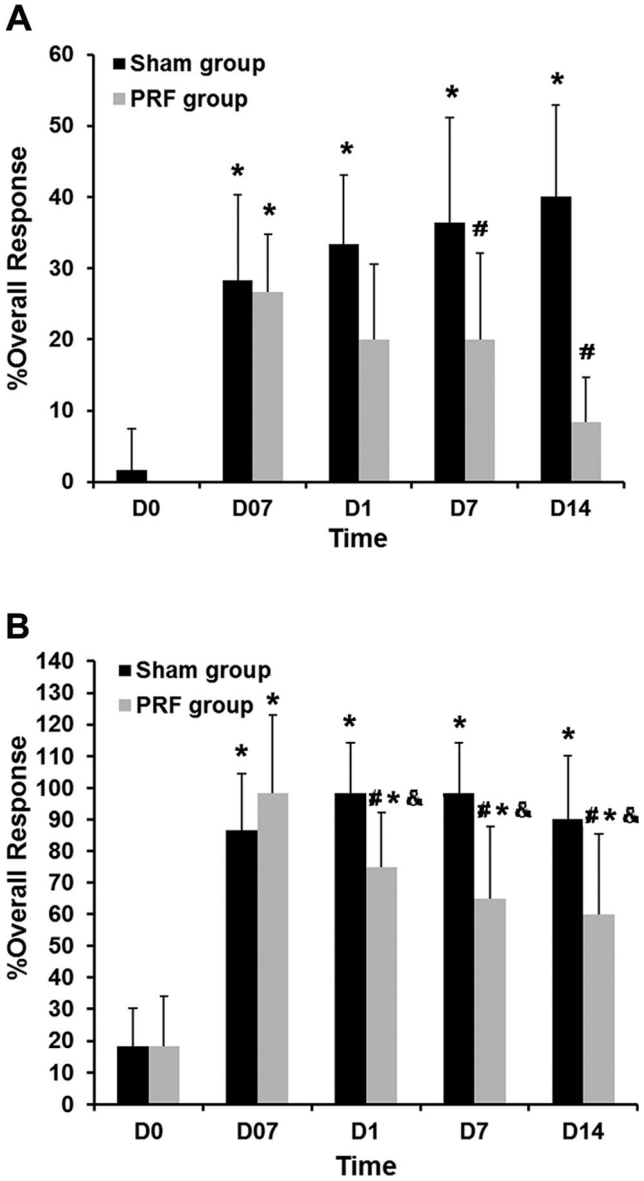

Fig. 3 Comparison of pain withdrawal threshold (PWT) in response to mechano-stimulation between rats in the PRF and Sham groups (n=12 for each group). **a** The mean response frequency to 4 g mechanical stimulation was near 0 % before surgery (D0), but rose after CCI (D07), indicating mechano-allodynia. This allodynia was progressively reversed in the PRF group, but was sustained in the Sham group (D1–D14). **b** The mean response frequency to stimulation with a 15 g von Frey filament increased significantly after CCI in both groups (D07). After PRF, the response decreased gradually in the PRF group, indicating partial reversal of mechano-hyperalgesia, but remained elevated in the Sham group. Data are presented as the mean±SEM. $^{\#}P<0.05$, PRF group vs. the sham group at each time point using mixed-effects REML regression; $^{*}P<0.005$ within groups compared with D0 using mixed-effects REML regression, adjusted using Bonferroni multiple comparison correction; &$P<0.005$ within groups compared with D07 using mixed-effects REML regression, adjusted using Bonferroni multiple comparison correction.

points, compared with D07 values ($P>0.005$, Figs. 4 and 5). In contrast, PRF treatment resulted in a gradual increase of HCN1 and HCN2 expression thereafter (Figs. 4 and 5).

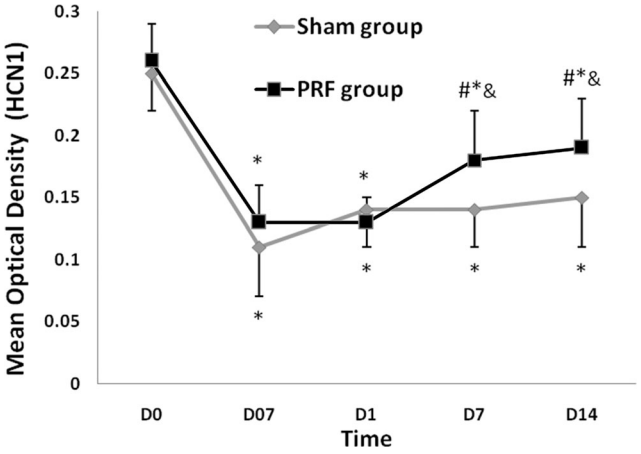

Fig. 4 The expression of HCN1 in DRG neurons of rats in the Sham (D0, D07, D1, D7, and D14) and PRF (D0, D07, D1, D7, and D14) groups, investigated by immunocytochemistry (×100; scale bars, 100 μm). Representative images are shown; in each group at each time point, the results were similar in all six rats investigated. HCN1-immunoreactivity was detected on all DRG neurons, mainly on the plasma membrane of large- and medium-sized DRG neurons. The *arrows* demarcate immunopositive cells. Immunoreactivity (staining intensity) was substantially reduced by CCI in both groups. Following PRF or Sham treatment, immunoreactivity gradually increased in DRG sections from rats in the PRF group, but remained low in those in the Sham group. Immunohistochemistry results were quantified. $^{\#}P<0.05$, PRF group vs. the sham group at each time point using mixed-effects REML regression; $^{*}P<0.005$ within groups compared with D0 using mixed-effects REML regression, adjusted using the Bonferroni multiple comparison correction; &$P<0.005$ within groups compared with D07 using mixed-effects REML regression, adjusted using Bonferroni multiple comparison correction

Precisely, at days 7 (D7) and 14 (D14) after PRF treatment, HCN1 expression was significantly increased compared with that obtained for D07 ($P<0.005$), although still significantly lower than baseline values obtained at D0 ($P<0.005$, Fig. 4); HCN2 expression at D14 was significantly increased compared with D07 values ($P<0.005$), but significantly lower than what recorded for D0 ($P<0.005$). Of note, the expression levels of both HCN1 and HCN2 at D14 were significantly higher in the PRF group than in sham animals ($P<0.05$, Figs. 4 and 5).

HCN1 and HCN2 Protein Expression after Nerve Injury

Western blotting and densitometric analyses were performed to quantify the changes in HCN1 and HCN2 expression levels in DRG neurons. The expression levels of HCN1 and HCN2 did not differ between the two groups of rats at baseline (D0) and decreased significantly ($P<0.005$) in both groups following CCI (Figs. 6 and 7). After PRF (D1–D14), HCN1 protein expression was significantly higher at D7 and D14 compared to D7, but was still lower at D14 than at baseline ($P<0.005$) (Fig. 6). Expression of HCN1 protein also increased in the Sham group and was significantly higher at D7 and D14 compared to D07 ($P<0.005$) (Fig. 6). However, HCN1 expression

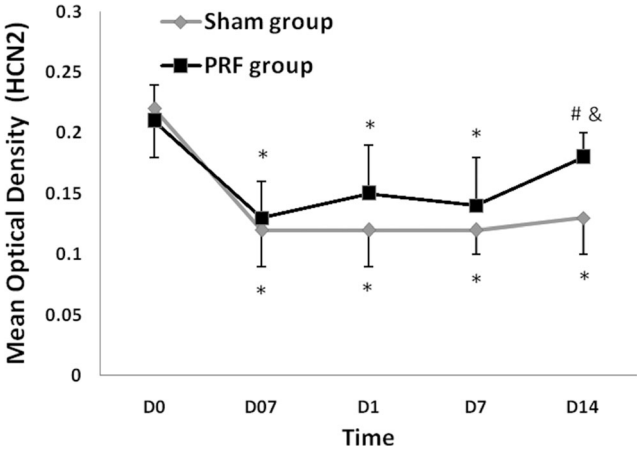

Fig. 5 The expression of HCN2 in DRG neurons of rats in the Sham (D0, D07, D1, D7, and D14) and PRF (D0, D07, D1, D7, and D14) groups, investigated by immunocytochemistry (×100; scale bars, 100 μm). Representative images are shown; in each group at each time point, the results were similar in all six rats investigated. HCN1-immunoreactivity was detected on all DRG neurons, mainly on the plasma membrane of large- and medium-sized DRG neurons. The *arrows* demarcate immunopositive cells. Immunoreactivity (staining intensity) was substantially reduced by CCI in both groups. Following PRF or sham treatment, immunoreactivity gradually increased in DRG sections from rats in the PRF group, but remained low in those in the Sham group. Immunohistochemistry results were quantified. $^{\#}P<0.05$, PRF group vs. the sham group at each time point using mixed-effects REML regression; $^{*}P<0.005$ within groups compared with D0 using mixed-effects REML regression, adjusted using Bonferroni multiple comparison correction; $\&P<0.005$ within groups compared with D07 using mixed-effects REML regression, adjusted using Bonferroni multiple comparison correction

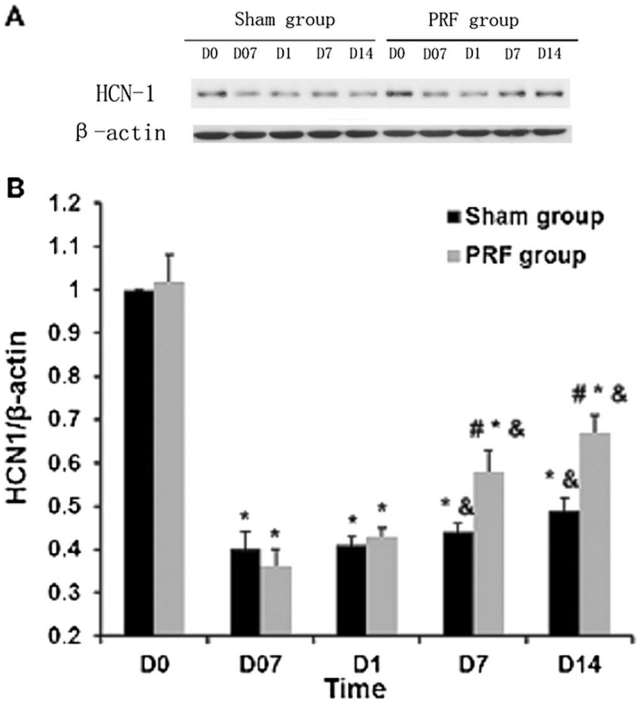

Fig. 6 Western blot analysis of HCN1 channel protein expression in DRG neurons (n=6 per group). **a** Sample blot showing representative results. HCN1 protein content decreased after nerve injury in both groups (D07 vs. D0). **b** Mean densitometry data (expressed relative to β-actin). After PRF (from D1 to D14), protein expression rose gradually in both groups, but was higher in the PRF group at D1, D7, and D14. Data are expressed as the mean±SEM. $^{\#}P<0.05$, PRF group vs. the sham group at each time point using mixed-effects REML regression; $^{*}P<0.005$ within groups compared with D0 using mixed-effects REML regression, adjusted using Bonferroni multiple comparison correction; $\&P<0.005$ within groups compared with D07 using mixed-effects REML regression, adjusted using Bonferroni multiple comparison correction

at D7 and D14 was significantly higher in the PRF group than in the Sham group ($P<0.05$) (Fig. 6). Thus, PRF enhanced the recovery of HCN1 expression following CCI. Similar results were observed for HCN2, except that HCN2 expression in the PRF group was higher than that of in the Sham group for all posttreatment days ($P<0.05$) (Fig. 7).

Discussion

The main findings of the present study were that CCI to the rat sciatic nerve downregulated the expression of HCN1 and HCN2 in L4–L6 DRG, which contain the cell bodies of the majority of sciatic nerve axons, and that alleviation of the CCI-induced thermo- and mechano-hyperalgesia by PRF treatment was associated with an upregulation of HCN1 and HCN2. These novel findings implicate changes in HCN channel expression in PRF neuromodulation.

One of the first proposals for the efficacy of PRF was tissue thermal coagulation; however, later studies demonstrated that the clinical effects of PRF against neuropathic pain do not rely on thermal injury (Podhajsky et al. 2005). The current view is that electromagnetic fields generated by PRF can alter neuronal gene expression (Hamann et al. 2006). Zundert et al. found that PRF upregulates c-fos and downstream genes in spinal dorsal horn neurons (Van Zundert et al. 2003), while Hamann et al. reported upregulated expression of ATF-3, another widely expressed transcription factor, after PRF (Hamann et al. 2006). Hagiwara et al. demonstrated that PRF prevents the chemically-induced decrease in norepinephrine-mediated spinal pain inhibition and enhances serotonin-mediated spinal pain inhibition (Hagiwara et al. 2009), suggesting that PRF alters genes controlling monoaminergic neuron function or neurotransmission.

In addition to the relevance of genes controlling neurotransmission, changes in PNS ion channel gene expression, including HCN genes, may also play a crucial role in the development and reversal of neuropathic pain. HCN channels mediating Ih are closely associated with neuropathic pain (Chaplan et al. 2003; Jiang et al. 2008; Wickenden et al. 2009; Mazo et al. 2013). Indeed, nerve injury has been reported to increase pacemaker currents in large DRG neurons, leading to spontaneous action potentials in the ligated nerve, while blockade of HCNs has been found to reverse injury-

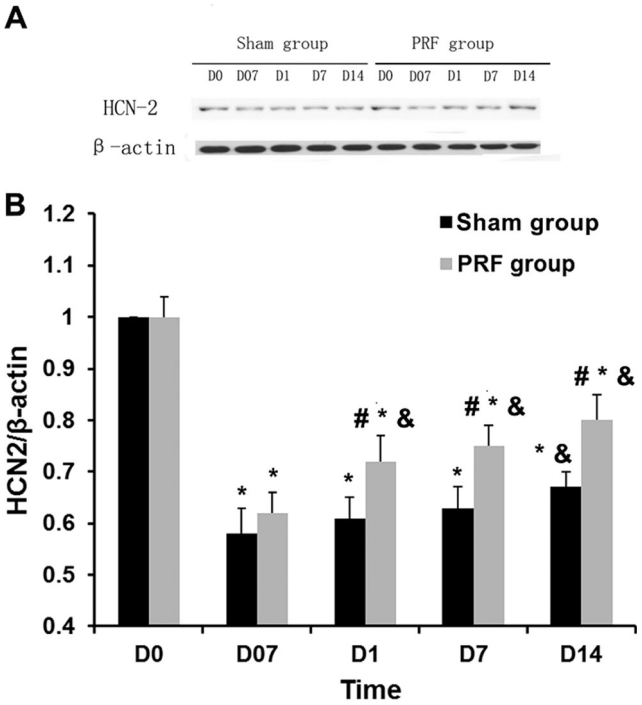

Fig. 7 Western blot analysis of HCN2 channel protein expression in DRG neurons (n=6 per group). **a** Sample blot showing representative results. HCN2 protein content decreased after nerve injury in both groups (D07 vs. D0). **b** Mean densitometry data (expressed relative to β-actin). After PRF (from D1 to D14), protein expression rose gradually in both groups but was higher in the PRF group at D7 and D14. Data are expressed as the mean±SEM. $^{\#}P<0.05$, PRF group vs. the sham group at each time point using mixed-effects REML regression; $^{*}P<0.005$ within groups compared with D0 using mixed-effects REML regression, adjusted using Bonferroni multiple comparison correction; $\&P<0.005$ within groups compared with D07 using mixed-effects REML regression, adjusted using Bonferroni multiple comparison correction

induced hyperalgesia (Chaplan et al. 2003). Four mammalian HCN channels have been cloned, HCN1–4, and subsequent studies have demonstrated widespread expression of all isoforms in both the PNS and CNS (Ludwig et al. 1998). Changes in DRG neurons, the primary sensory neurons in peripheral pain processing, are crucial for the development of neuropathic pain (Chung et al. 2002; Sluijter 2005; Wan 2008; Perret et al. 2011). The present study revealed differential expression of HCN channel subtypes in DRG neurons, with HCN1 expressed mainly on the plasma membrane of large and medium-sized neurons, and HCN2 mainly in the cytoplasm of medium and small-sized neurons. The distribution and functions of HCN3 and HCN4 in the DRG remain largely unknown; since both these isoforms have been reported to be expressed weakly in normal and pathologic DRG (Moosmang et al. 2001; Jiang et al. 2008), our study focused on CCI- and PRF-induced changes in the expression levels of HCN1 and HCN2.

The main findings of the present study regarding HCN channel expression appear, at face value, to be in contradiction to the previous investigations. Du et al. have observed that increased expression of HCN1 and HCN2 and a shift in the activation curve of Ih occur in a rat model of neuropathic pain (Du et al. 2013a, b). The activity of HCN1 is repressed by analgesics, while knockout of HCN2 abolishes neuropathic pain in response to nerve injury in mice (Emery et al. 2011; Emery et al. 2012; Tibbs et al. 2013). Xie et al. observed increased Ih in primary afferent neurons of rats with nerve CCI-induced spontaneous pain (Xie et al. 2005). Dalle et al. reported that blockade of Ih in peripheral neurons of rats with partial SNL alleviated mechano-allodynia (Dalle et al. 2005), while other studies in animal models of neuropathic pain have also observed reductions in mechanical allodynia and thermal hyperalgesia with pharmacologic inhibition of Ih (Du et al. 2013a; Tibbs et al. 2013; Young et al. 2014). Wickenden et al. found that HCN channels in medium and large-sized DRG neurons of injured primary sensory nerves responded preferentially to nociceptive discharges (Wickenden et al. 2009). While these various studies suggest that HCNs promote neuropathic pain, several investigators have provided evidence that changes in HCN channel expression do not correlate well with Ih density. Chaplan et al. found that nerve injury markedly increased Ih in DRG neurons of rats with SNL, but (consistent with our observations) decreased HCN1 and HCN2 mRNA and protein expression (Chaplan et al. 2003). Jiang et al. also found increased Ih in the DRG of rats with nerve CCI, but a slight reduction in HCN1 and HCN2 expression levels in large DRG neurons (Jiang et al. 2008). Therefore, the increase in Ih current density, observed following nerve injury, may not be attributable to an increase in HCN channel protein expression. Instead, these results suggest that changes in Ih associated with neuropathic pain are secondary to posttranslational modifications to HCN channels. A large variety of mechanisms might contribute to HCN channel regulation, including transcriptional control, trafficking, channel assembly, and modification by intracellular and extracellular factors such as numerous kinases, MinK-related protein (MiRP1), KCR1, neuronal scaffold proteins, filamin A, caveolin-3, acidic lipids, protons, and chloride (Biel et al. 2009; He et al. 2014). In the present study, it was notable that HCN2 channels were expressed mainly in the cytoplasm rather than the plasma membrane; however, Ih density will be dependent on the number of functional channels in the plasma membrane and the electrophysiological properties of these channels (determined, in part, through modulation of the channels by interacting factors and kinases), rather than on the total number of expressed proteins. Thus, the changes in HCN channel expression determined in the present study may not actually reflect the alterations in Ih current density, and indeed may even be compensatory changes occurring in the opposite direction to the alteration in functional Ih current. It is also relevant that the present study determined changes in HCN channel expression in the somata of damaged DRG neurons and not in the axons; it remains possible that changes

in the axonal expression of HCN channels may have differed from those of the somata and that the axonal changes exerted the major influence on nociceptive transmission.

In this study, HCN channel expression was reduced in DRG neurons after sciatic nerve CCI, in accordance with the previous studies (Chaplan et al. 2003; Jiang et al. 2008). Expression of HCN1 and HCN2 increased in both groups between D07 and D1, indicative of spontaneous upregulation, but this upregulation was significantly faster in the PRF group. Furthermore, in the PRF group, there was a concomitant reversal in CCI-induced thermo- and mechano-hyperalgesia, suggesting reduced spontaneous activity in DRG neurons. We speculate that the HCN upregulation in the Sham group may reflect nerve recovery over time. However, there was a disconnection between HCN channel expression and behavioral responses to pain in the two groups. In the Sham group, the increase in HCN1 and HCN2 expression levels was associated with shorter thermal withdrawal latency and lower mechanical withdrawal threshold (i.e., signs of greater neuropathic pain), while PRF-treated rats exhibited the converse relationship. Obviously, changes in neuropathic pain during recovery reflect many simultaneous compensatory and pathologic alterations in addition to changes in HCN1/2 expression. By D14, the expression of HCN channels had increased in both groups, but was significantly higher in the PRF group, indicating that PRF can affect the expression of HCN channels in the DRG. In general, PRF suppressed behavioral correlates of neuropathic pain. We speculate that HCN1/2 expression regulates neuropathic pain, but that posttranslational modulation of HCN channel activity may exert an even more important influence on neuropathic pain. Additional studies are required to elucidate the precise mechanisms by which HCN channel expression and function contribute to neuropathic pain and the benefits of therapeutic interventions such as PRF.

There were a few limitations to our study. We focused only on the expression of HCN channels and did not assess their function (such as Ih density). Spontaneous DRG activity was assessed indirectly through behavioral changes. Mechano-hyperalgesia and mechano-allodynia decreased after PRF, suggesting a decrease in spontaneous activity. In view of the inconsistent relationship between channel protein expression and Ih, future studies should assess the effect of PRF on Ih current density in DRG neurons. Moreover, we determined changes in HCN channel expression only in the somata of damaged neurons (in the DRG); it cannot be excluded that alterations in the axonal expression of HCN channels may have affected nociceptive transmission.

In conclusion, we established a rat model of neuropathic pain, using sciatic nerve CCI, to study the effects of PRF on HCN channel expression in DRG neurons. PRF enhanced the expression of HCN1 and HCN2 in DRG neurons and reversed post-CCI hyperalgesia. These results further confirm the anti-nociceptive efficacy of PRF in rats with sciatic nerve CCI and implicate changes in HCN channel expression in PRF neuromodulation. Elucidating the precise role of HCN channels in neuropathic pain and in the beneficial effects of PRF will require detailed electrophysiological analyses of Ih currents.

Acknowledgments This study was supported by Peking University People's Hospital Research and Development Funds.

Conflict of Interest The authors declare that they have no competing interests.

References

Aksu R, Ugur F, Bicer C et al (2010) The efficiency of pulsed radiofrequency application on L5 and l6 dorsal roots in rabbits developing neuropathic pain. Reg Anesth Pain Med 35(1):11–15

Bennett GJ, Xie YK (1988) A peripheral mononeuropathy in rat that produces disorders of pain sensation like those seen in man. Pain 33(1):87–107

Biel M, Wahl-Schott C, Michalakis S, Zong X (2009) Hyperpolarization-activated cation channels: from genes to function. Physiol Rev 89(3):847–885

Chaplan SR, Guo HQ, Lee DH et al (2003) Neuronal hyperpolarization-activated pacemaker channels drive neuropathic pain. J Neurosci 23(4):1169–1178

Chung JM, Chung K (2002) Importance of hyperexcitability of DRG neurons in neuropathic pain. Pain Pract 2(2):87–97

Cohen SP, Sireci A, Wu CL, Larkin TM, Williams KA, Hurley RW (2006) Pulsed radiofrequency of the dorsal root ganglia is superior to pharmacotherapy or pulsed radiofrequency of the intercostal nerves in the treatment of chronic postsurgical thoracic pain. Pain Physician 9(3):227–235

Dalle C, Eisenach JC (2005) Peripheral block of the hyperpolarization-activated cation current (Ih) reduces mechanical allodynia in animal models of postoperative and neuropathic pain. Reg Anesth Pain Med 30(3):243–248

Du L, Wang SJ, Cui J, He WJ, Ruan HZ (2013a) Inhibition of HCN channels within the periaqueductal gray attenuates neuropathic pain in rats. Behav Neurosci 127(2):325–329

Du L, Wang SJ, Cui J, He WJ, Ruan HZ (2013b) The role of HCN channels within the periaqueductal gray in neuropathic pain. Brain Res 150036-44

Emery EC, Young GT, Berrocoso EM, Chen L, McNaughton PA (2011) HCN2 ion channels play a central role in inflammatory and neuropathic pain. Science 333(6048):1462–1466

Emery EC, Young GT, McNaughton PA (2012) HCN2 ion channels: an emerging role as the pacemakers of pain. Trends Pharmacol Sci 33(8):456–463

Flatters SJ, Bennett GJ (2004) Ethosuximide reverses paclitaxel- and vincristine-induced painful peripheral neuropathy. Pain 109(1-2): 150–161

Hagiwara S, Iwasaka H, Takeshima N, Noguchi T (2009) Mechanisms of analgesic action of pulsed radiofrequency on adjuvant-induced pain in the rat: Roles of descending adrenergic and serotonergic systems. Eur J Pain 13(3):249–252

Hains BC, Saab CY, Klein JP, Craner MJ, Waxman SG (2004) Altered sodium channel expression in second-order spinal sensory neurons contributes to pain after peripheral nerve injury. J Neurosci 24(20): 4832–4839

Hamann W, Abou-Sherif S, Thompson S, Hall S (2006) Pulsed radiofrequency applied to dorsal root ganglia causes a selective increase in ATF3 in small neurons. Eur J Pain 10(2):171–176

Hargreaves K, Dubner R, Brown F, Flores C, Joris J (1988) A new and sensitive method for measuring thermal nociception in cutaneous hyperalgesia. Pain 32(1):77–88

Hatch RJ, Jennings EA, Ivanusic JJ (2013) Peripheral hyperpolarization-activated cyclic nucleotide-gated channels contribute to inflammation-induced hypersensitivity of the rat temporomandibular joint. Eur J Pain 17(7):972–982

He C, Chen F, Li B, Hu Z (2014) Neurophysiology of HCN channels: from cellular functions to multiple regulations. Prog Neurobiol 1121-23

Jiang YQ, Xing GG, Wang SL et al (2008) Axonal accumulation of hyperpolarization-activated cyclic nucleotide-gated cation channels contributes to mechanical allodynia after peripheral nerve injury in rat. Pain 137(3):495–506

Ke M, Yinghui F, Yi J et al (2013) Efficacy of pulsed radiofrequency in the treatment of thoracic postherpetic neuralgia from the angulus costae: a randomized, double-blinded, controlled trial. Pain Physician 16(1):15–25

Kerstman E, Ahn S, Battu S, Tariq S, Grabois M (2013) Neuropathic pain. Handb Clin Neurol 110175-187

Li CY, Song YH, Higuera ES, Luo ZD (2004) Spinal dorsal horn calcium channel alpha2delta-1 subunit upregulation contributes to peripheral nerve injury-induced tactile allodynia. J Neurosci 24(39):8494–8499

Ludwig A, Zong X, Jeglitsch M, Hofmann F, Biel M (1998) A family of hyperpolarization-activated mammalian cation channels. Nature 393(6685):587–591

Mazo I, Rivera-Arconada I, Roza C (2013) Axotomy-induced changes in activity-dependent slowing in peripheral nerve fibres: Role of hyperpolarization-activated/HCN channel current. Eur J Pain 17(9):1281–1290

Moosmang S, Stieber J, Zong X, Biel M, Hofmann F, Ludwig A (2001) Cellular expression and functional characterization of four hyperpolarization-activated pacemaker channels in cardiac and neuronal tissues. Eur J Biochem 268(6):1646–1652

Park HW, Ahn SH, Son JY et al (2012) Pulsed radiofrequency application reduced mechanical hypersensitivity and microglial expression in neuropathic pain model. Pain Med 13(9):1227–1234

Perret DM, Kim DS, Li KW et al (2011) Application of pulsed radiofrequency currents to rat dorsal root ganglia modulates nerve injury-induced tactile allodynia. Anesth Analg 113(3):610–616

Podhajsky RJ, Sekiguchi Y, Kikuchi S, Myers RR (2005) The histologic effects of pulsed and continuous radiofrequency lesions at 42 degrees C to rat dorsal root ganglion and sciatic nerve. Spine (Phila Pa 1976) 30(9):1008–1013

Postea O, Biel M (2011) Exploring HCN channels as novel drug targets. Nat Rev Drug Discov 10(12):903–914

Sluijter ME (2005) Pulsed radiofrequency. Anesthesiology 103(6):1313, **author reply 1313-1314**

Tanaka N, Yamaga M, Tateyama S, Uno T, Tsuneyoshi I, Takasaki M (2010) The effect of pulsed radiofrequency current on mechanical allodynia induced with resiniferatoxin in rats. Anesth Analg 111(3):784–790

Tibbs GR, Rowley TJ, Sanford RL et al (2013) HCN1 channels as targets for anesthetic and nonanesthetic propofol analogs in the amelioration of mechanical and thermal hyperalgesia in a mouse model of neuropathic pain. J Pharmacol Exp Ther 345(3):363–373

Van Zundert J, Brabant S, Van de Kelft E, Vercruyssen A, Van Buyten JP (2003) Pulsed radiofrequency treatment of the Gasserian ganglion in patients with idiopathic trigeminal neuralgia. Pain 104(3):449–452

Vranken JH (2012) Elucidation of pathophysiology and treatment of neuropathic pain. Cent Nerv Syst Agents Med Chem 12(4):304–314

Wan Y (2008) Involvement of hyperpolarization-activated, cyclic nucleotide-gated cation channels in dorsal root ganglion in neuropathic pain. Sheng Li Xue Bao 60(5):579–580

Wickenden AD, Maher MP, Chaplan SR (2009) HCN pacemaker channels and pain: a drug discovery perspective. Curr Pharm Des 15(18):2149–2168

Xiao J, Nguyen TV, Ngui K et al (2004) Molecular and functional analysis of hyperpolarisation-activated nucleotide-gated (HCN) channels in the enteric nervous system. Neuroscience 129(3):603–614

Xie W, Strong JA, Meij JT, Zhang JM, Yu L (2005) Neuropathic pain: Early spontaneous afferent activity is the trigger. Pain 116(3):243–256

Young GT, Emery EC, Mooney ER, Tsantoulas C, McNaughton PA (2014) Inflammatory and neuropathic pain are rapidly suppressed by peripheral block of hyperpolarisation-activated cyclic nucleotide-gated ion channels. Pain 155(9):1708–1719